Enzymatically enhanced collisions on ultramicroelectrodes for specific and rapid detection of individual viruses

Jeffrey E. Dick[a,1], Adam T. Hilterbrand[b,1], Lauren M. Strawsine[a], Jason W. Upton[b], and Allen J. Bard[a,2]

[a]Center for Electrochemistry, Department of Chemistry, The University of Texas at Austin, Austin, TX 78712; and [b]Department of Molecular Biosciences, LaMontagne Center for Infectious Disease, and Institute for Cellular and Molecular Biology, The University of Texas at Austin, Austin, TX 78712

We report the specific collision of a single murine cytomegalovirus (MCMV) on a platinum ultramicroelectrode (UME, radius of 1 µm). Antibody directed against the viral surface protein glycoprotein B functionalized with glucose oxidase (GOx) allowed for specific detection of the virus in solution and a biological sample (urine). The oxidation of ferrocene methanol to ferrocenium methanol was carried out at the electrode surface, and the ferrocenium methanol acted as the cosubstrate to GOx to catalyze the oxidation of glucose to gluconolactone. In the presence of glucose, the incident collision of a GOx-covered virus onto the UME while ferrocene methanol was being oxidized produced stepwise increases in current as observed by amperometry. These current increases were observed due to the feedback loop of ferrocene methanol to the surface of the electrode after GOx reduces ferrocenium methanol back to ferrocene. Negative controls (i) without glucose, (ii) with an irrelevant virus (murine gammaherpesvirus 68), and (iii) without either virus do not display these current increases. Stepwise current decreases were observed for the prior two negative controls and no discrete events were observed for the latter. We further apply this method to the detection of MCMV in urine of infected mice. The method provides for a selective, rapid, and sensitive detection technique based on electrochemical collisions.

collisions | cytomegalovirus | electrochemistry | electrovirology | ELISA

The development of methods to observe collisions on ultramicroelectrodes (UMEs) has allowed for the study of single entities, such as single nanoparticles (1), emulsion droplets (2, 3), vesicles (4, 5), biological macromolecules (6), and even single ions (7), in a digital manner (8). However, many of the techniques developed lack specificity. In the field of collisions, the study of biologically relevant analytes of interest, such as viruses and cells, has been largely unexplored. Perhaps the greatest challenges in these experiments are achieving specificity and understanding the electrochemical response. Overcoming these challenges will ultimately lead to the development of sensitive detection methodologies based on facile and inexpensive electrochemical methods, which will be of importance in the diagnosis of infectious diseases.

Rapid, accurate diagnosis is a critical first step in the care of those suffering from viral infections. ELISAs, PCR-based techniques, or culture methods are fairly reliable diagnostic measures with varying degrees of sensitivity (9–11). However, these diagnostic techniques require a significant degree of sample and experimental preparation, increasing the amount of time between a positive diagnosis and the beginning of treatment. Diagnostic tools that are able to directly sample from complex media (i.e., blood, serum, urine, etc.) are necessary to expedite the diagnostic process.

One such infectious agent that requires rapid and early detection is human cytomegalovirus (HCMV). HCMV is a prototypical betaherpesvirus, establishing lifelong latent infections in its host. In developing countries, nearly 100% of adults have this virus, and 50% of adults are infected in developed nations (12). Although immunocompetent individuals typically remain unsymptomatic upon HCMV infection, those who are immunodeficient or naïve, such as transplant recipients or newborn children, are more likely to display

symptoms of infection. Typically, reliable diagnosis of primary HCMV infection relies on the detection of HCMV DNA or culture methods. Current or previous exposure to HCMV can be detected by the identification of circulating IgM or IgG antibodies specific for HCMV (13). These diagnostic procedures can be invasive, requiring the drawing of blood or amniotic fluid for fetal testing, and they can require lengthy and tedious sample preparation. Hence, it is necessary to develop analytical methodologies that allow for the rapid and specific detection of HCMV in urine or saliva samples. Urinalysis for the presence of HCMV provides a noninvasive means for primary HCMV diagnosis. Furthermore, electrochemistry is an apt analytical tool for the detection of biologically relevant analytes of interest, as demonstrated by the utility of glucometers (14). In this paper, we present a step forward in the field of nanoelectrochemistry that represents a preliminary step toward an inexpensive and facile electrochemical method for detecting specific viruses.

Previously, we reported the electrochemical detection of murine cytomegalovirus (MCMV) collisions on an UME (15). The anatomy of the virus is outlined in Fig. 1A. In this previous study, while a reaction was being carried out at the electrode surface, MCMV adsorbed nonspecifically to the electrode surface, effectively blocking the reaction. This behavior, so-called blocking, manifested itself as a stepwise current decrease in the amperometric response. To gain specificity, virus was incubated with an antibody (anti-gB) specific for the virion surface protein, glycoprotein B (gB), and polystyrene beads (PSBs) functionalized with a secondary antibody specific to the Fc region of the anti-gB antibody. In the presence of MCMV, these functionalized PSBs agglomerated, which manifested itself as a
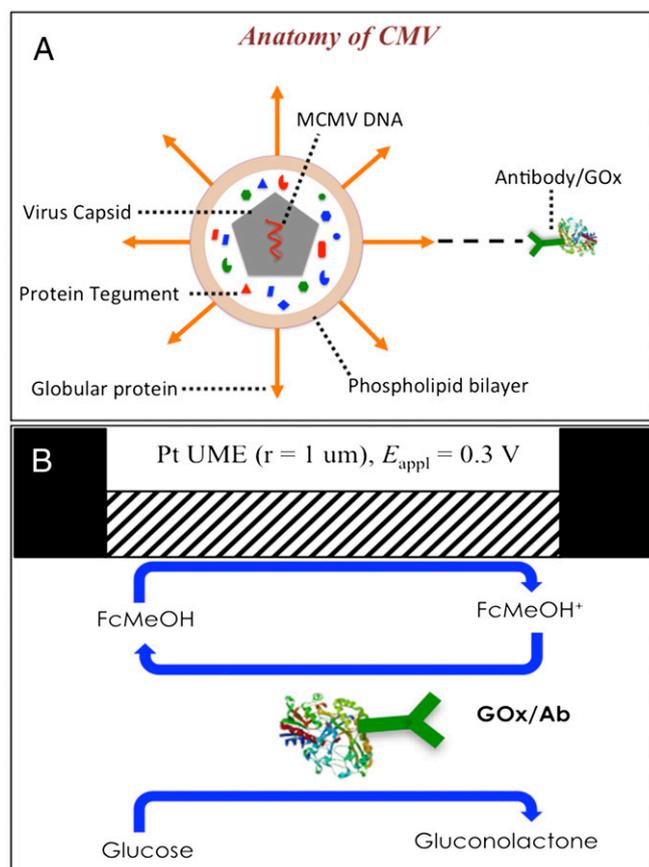
CHEMISTRY

MICROBIOLOGY

Fig. 1. (*A*) Schematic representation of the CMV virion and corresponding antibody/GOx interaction with a surface glycoprotein. (*B*) Schematic representation of the antibody and GOx conjugate regenerating ferrocene methanol from ferrocenium methanol, the latter of which is continuously replenished via oxidation at an electrode surface, in the presence of glucose. The figure is not drawn to scale.

decrease of collision frequency of PSBs in amperometry. In the rare event that a larger aggregate collided with the electrode surface, a larger stepwise decrease in current was observed. Even with the large aggregates, collisions were recorded in intervals on the order of minutes.

In this paper, we have extended the collision of single viruses to a more specific analytical technique via enzymatic labeling. Glucose oxidase (GOx) catalyzes the oxidation of glucose to gluconolactone while reducing an oxidant molecule, such as ferrocenium methanol. When oxygen is removed from solution, and the oxidation of ferrocene methanol to ferrocenium methanol is carried out at the electrode surface, the electrons from the glucose oxidation will reduce ferrocenium back to ferrocene, and feedback will be detected at the electrode surface, as shown in Fig. 1*B* (16). This chemistry is similar to the chemistry used in usual glucometers (14). This local feedback of ferrocene to the electrode surface causes an increase in the current response. Because the environmental noise of most potentiostats is on the order of 10–100 fA, and a single faradaic enzyme collision is capable of generating *ca.* 0.2 fA of current (17), single faradaic enzyme collisions cannot be discerned against the background. Hence, a single enzyme on an electrode surface cannot produce enough current to discern against the background. However, by covalently attaching GOx to a specific antibody, which in turn binds to epitopes around the virus, GOx can be specifically concentrated on the virus surface, thereby significantly amplifying the signal to produce positive current steps able to be detected on conventional potentiostats.

As shown in Fig. 2*A*, the virus itself will nonspecifically adsorb to the electrode surface, effectively blocking the redox reaction being carried out. Fig. 2*B* gives the expected amperometric response for this blocking experiment. In Fig. 2*C*, GOx-labeled anti-gB antibody binds the surface of MCMV in solution, allowing the virus to preconcentrate thousands of enzymes for detection at the electrode surface, greatly amplifying the signal of just one GOx enzyme. The predicted amperometric response when the virus is surrounded by GOx is shown in Fig. 2*D*. If the conjugation is incomplete or the antibody is not specific to the virus, no preconcentration occurs, and blocking will be observed, consistent with numerous examples of blocking in the literature (18–20). When the virus carries thousands of GOx enzymes to the electrode, feedback is generated, creating a discrete, positive current response.

Results

Collisions of Antibody/GOx-Coated MCMV. Fig. 3 shows the amperometric i-t response for the collisions of virus after incubation in the antibody/GOx solution in the presence of 1 mM ferrocene methanol and 50 mM glucose. The background current of about 348 pA is from the oxidation of ferrocene methanol to ferrocenium methanol. From the amperometric response, positive current steps with a slight deactivation are realized (anodic current is plotted negatively). The decay of the catalytic current is likely due to nonspecific adsorption of organic molecules, such as proteins and/or lipids, onto the electrode surface, blocking ferrocene oxidation sites. In the absence of virus, there is not enough buildup of GOx to cause a discrete event. The current steadily increased over time due to nonspecific adsorption of the GOx/Ab conjugate on the electrode surface (*SI Appendix,* Fig. S1). No discrete steps were seen because one GOx enzyme is not able to generate enough current to manifest as a discrete event. A table summarizing the type of events observed (blocking or catalytic amplification) is also given in *SI Appendix*. The frequency of the positive current steps increases

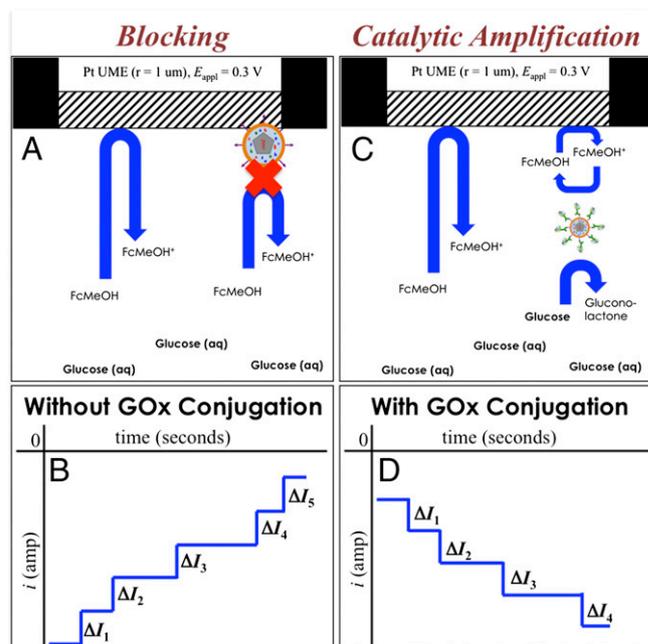**Fig. 2.** (*A*) Schematic representation of the collisions without conjugation to GOx. (*B*) Predicted amperometric response without conjugation. Stepwise decreases in current are expected. Anodic (oxidative) current is plotted negatively. (*C*) Schematic representation of the feedback mechanism from a virus covered in GOx. (*D*) Predicted amperometric response with conjugation to GOx. *A* and *C* are not drawn to scale.
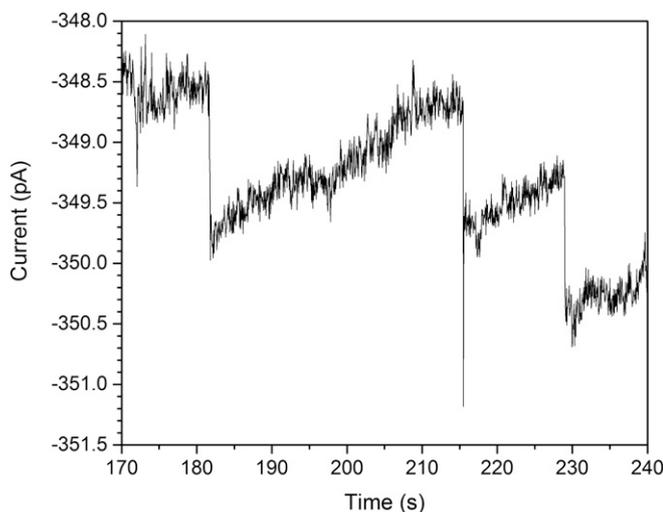
Fig. 3. Amperometric i-t response of the virus in the presence of the antibody/GOx conjugate. The purified virus was incubated with the GOx/antibody conjugate for 30 min before experimentation. Measurements were taken in 10 mM PBS, 1 mM ferrocene methanol, and 50 mM glucose on a 1-μm-radius Pt UME. The sampling rate for data acquisition was 50 ms.

linearly with the concentration of virus in solution (discussed below), indicating that these steps are due to collisions of MCMV.

From previous work by Savéant and coworkers, the current for a single GOx enzyme with ferrocenium methanol as the cosubstrate to the enzyme is ~0.2 fA (17, 18). The average current step height observed in the reported experiments was 0.8 ± 0.4 pA, implying that the amount of GOx enzyme on the virus surface is ~4,000, taking the current produced by one enzyme as 0.2 fA. By estimating the size of the conjugate as a 5- to 10-nm square, and taking the virus radius to be ~100 nm, the geometric capacity on the virus surface is between 1,300 and 5,000, which agrees with the electrochemical collision signal for a single virion. This estimate based on simple geometry does not consider the number of epitopes on the virus membrane or steric effects. We cannot completely rule out the possibility of the virus aggregating during incubation with the conjugate. From our previous study, virus aggregates were observed after adding PSBs functionalized with a secondary antibody specific to the primary antibody of MCMV, and we demonstrated that aggregates diffuse more slowly compared with free virus, colliding with the electrode at a lower frequency (16). In the studies presented here, current steps on the order of 4–6 pA, which could be interpreted as aggregates of virus, were infrequently observed in amperometry, occurring only three times in an analysis of over 80 anodic steps. It should be noted that these events were not counted during the statistical analysis of the anodic steps. Thus, although difficult to directly confirm, the results of our geometric analysis, coupled with the analysis of frequency of virus collisions (discussed belw), are consistent with detection of single MCMV virions in solution.

Discrimination of MCMV from Murine Gammaherpesvirus 68. To demonstrate specific discrimination of MCMV from other particles of similar size or morphology, experiments were carried out in the presence of MHV68, a murine gammaherpesvirus related to Epstein–Barr and Kaposi's sarcoma-associated herpesvirus. In the presence of anti-MCMV gB antibody/GOx conjugate, MHV68 shows only blocking at the electrode (Fig. 4A). This indicates that MHV68 does not preconcentrate GOx on its surface, because the epitope for the primary antibody is specific for MCMV gB and is in agreement with our previous work (16). When MHV68 and MCMV are assessed in a mixture of viruses in the presence of GOx–antibody conjugate, both blocking and positive current events are observed (Fig. 4B). Because positive current events only occur when MCMV preconcentrates

enough GOx by its highly specific antibody interaction, the presence of additional blocking events, presumably by MHV68 virions, demonstrates that MCMV can be detected in the presence of other viruses or solution species that nonspecifically adsorb to the electrode surface. The specificity of primary antibody allows for specific positive detection of MCMV by the electrochemical response.

Detection of MCMV in Urine of Infected Mice. To demonstrate the feasibility of this digital electrochemical collision technique to detection of virus in a biological sample, we applied our technique of MCMV detection in urine from an infected mouse at various times postinfection. Fig. 5A gives a schematic representation of the electrochemical immunoassay, and Fig. 5B emphasizes the detection of virus in the urine sample. Mice were infected with 10^6 pfu MCMV by i.p. injection, and urine was collected at times postinfection. Urine samples were incubated with antibody/GOx and subjected to amperometry. Fig. 5B shows representative results obtained 10 d
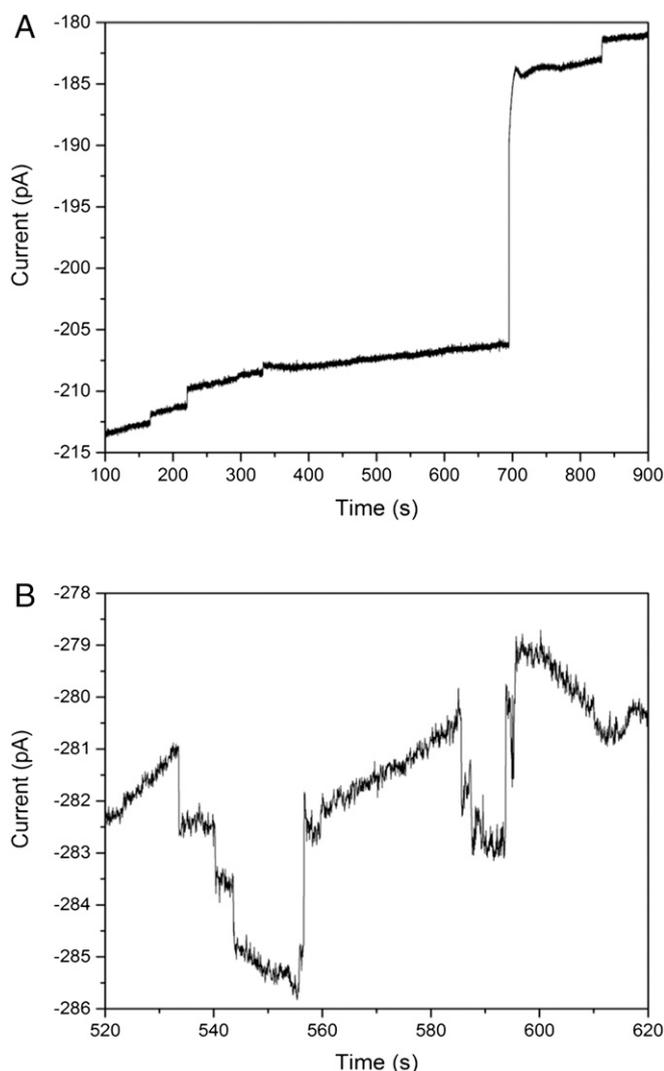
Fig. 4. (A) Amperometric i-t curve of MHV68 in the presence of the antibody/GOx conjugate with glucose in solution and 50 mM PBS. MHV68 blocks the flux of ferrocene methanol to the surface of the electrode. (B) Amperometric i-t curve of a mixture of MHV68 and MCMV with the antibody/GOx conjugate in a solution of 10 mM PBS, 50 mM glucose, and 1 mM ferrocene methanol showing positive and blocking current responses over the steady-state current level due to the collision of MCMV and MHV68, respectively. The steady-state current is the current due to the oxidation of ferrocene methanol on a 1-μm-radius Pt UME.
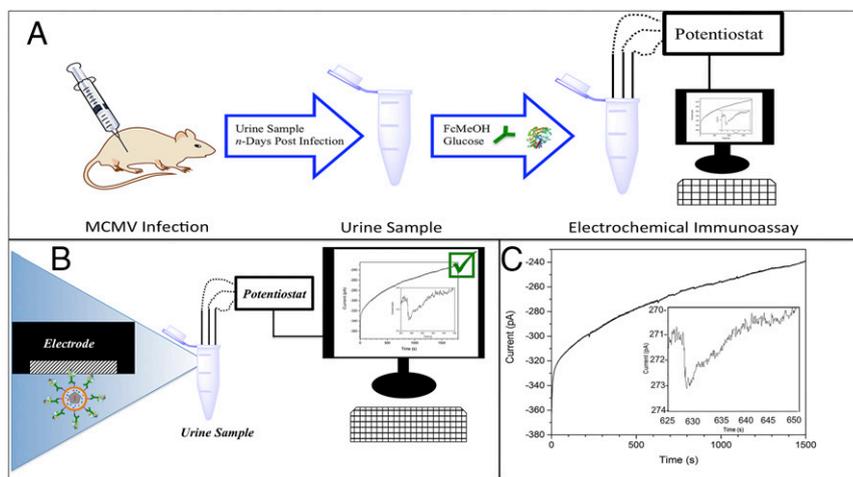
Fig. 5. (*A*) Schematic representation of the electrochemical immunoassay. (*B*) Enlargement of the assay emphasizing the detection of virus. (*C*) Representative amperometry of 50 μL urine diluted with 400 μL of 1 mM ferrocene methanol and 100 mM glucose with a representative enlargement of a positive response for a sample collected 10 d after the initial infection.

after the initial infection, and discrete positive current steps can be seen with a deactivation. The enlarged response shows the step-like nature of the discrete events observed in electrochemistry. Experiments with urine from an uninfected mouse showed no anodic step-like characteristics, indicating that a virus capable of concentrating GOx enzymes can only cause the positive anodic step. During experiments in urine in the absence of virus, a slow decay in the steady-state current was observed. This decay is likely due to non-specific adsorption of proteins and other organic species in urine that are not electrochemically active, as evidence by the deactivation. Upon collision, a virus covered in GOx will begin turning over ferrocenium to ferrocene, providing the feedback loop that gives the positive step in current. Due to nonspecific adsorption that is evident in the urine background current decay, likely from urea and other organic molecules found in urine, the feedback loop becomes less efficient, as emphasized in the enlarged portion of the amperometric i-t curve in Fig. 5*B*. However, positive current events can be detected, which demonstrates that this technique can be used to detect viruses in biological samples.

Discussion

The flux of biological species to the electrode surface can be modeled in a stochastic sense by considering the frequency with which a virus collides with the electrode depending on diffusion. This frequency, f^{dif}, is given by (21)

$$f^{dif} = 4DCaN_A,$$ [1]

where C is the concentration of virus in solution, a is the radius of the electrode, N_A is Avogadro's number, and D is the diffusion coefficient of a virus, given by the Stokes–Einstein relationship (22) below:

$$D = (k_B T) * (6\pi\eta r_v)^{-1},$$ [2]

where k_B is Boltzmann's constant, η is the viscosity of water, and r_V is the radius of the virus. From these two equations, the frequency is expected to vary linearly with the concentration of virus in solution.

Fig. 6 shows the frequency of anodic current events as a function of the concentration of MCMV for the experimental results (dashed line) and the calculated results (dotted line) from Eqs. **1** and **2**. The concentration of virus particles in solution was determined using nanoparticle tracking analysis (NTA), as previously described (16). The experimental curve has twice the slope of the calculated curve,

implying that mass transport to the electrode surface is not controlled only by diffusion. We have previously shown that the overall charge on the virus and virus with antibody is negative from investigations of zetapotential with NTA. When ferrocene is oxidized to ferrocenium at the electrode surface, a concentration gradient of positive charge is created. This positive gradient establishes an electrical field in which charged species can migrate. Because the virus and most biological species, such as cells and proteins, are negatively charged, they will be pulled to the electrode surface and increase the frequency of collision. The slope of the frequency versus concentration curve is higher for the control experiments in pure water, implying that migration likely plays a role in the mass transfer of the virus to the electrode surface. In the experiments with urine, the ionic strength of urine is greater than the control experiments in water with the virus. This means that the ions in the urine will carry a majority of the charge, and migration has less of a
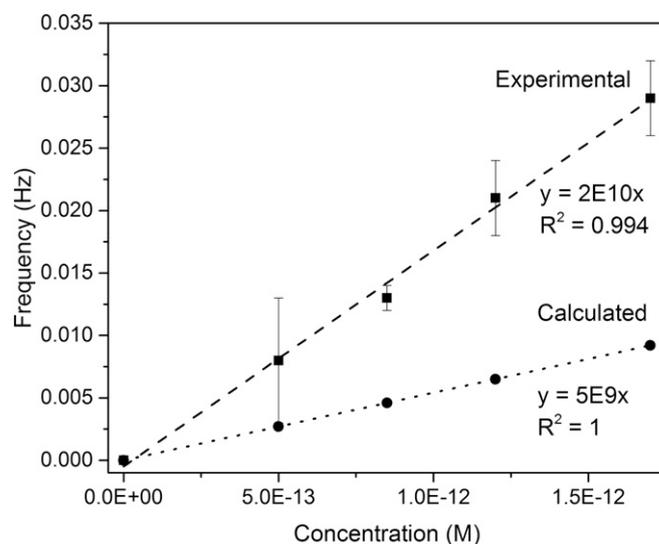

Fig. 6. Frequency of anodic steps as a function of concentration of MCMV for the experimental results (dashed line) plotted with the calculated expectation (dotted line), which assumes mass transfer only by diffusion. These experiments were carried out in 10 mM PBS. The SD was calculated from three independent experiments.
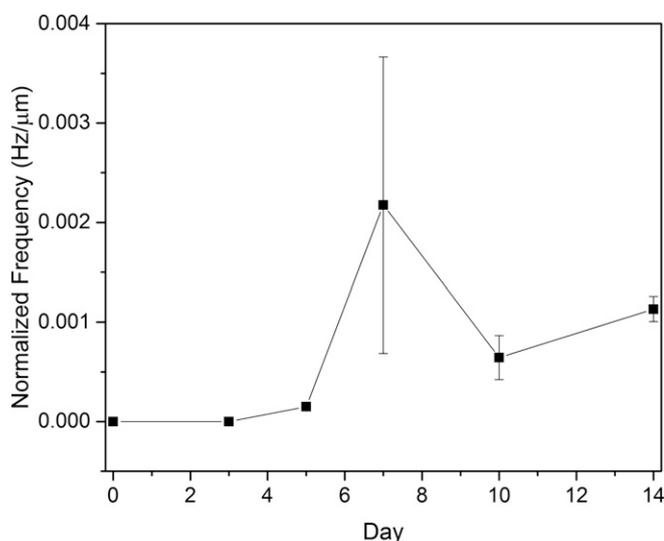
Fig. 7. Frequency of collision measured on a Pt UME (radius 1 μm) by diluting 50 μL infected mouse urine with 400 μL of a 1 mM FcMeOH and 50 mM glucose solution in urine as a function of days postinfection. The SD corresponds to 10 independent measurements: Two measurements over 2,000 s were taken for five different mice.

role in mass transfer. For the control experiments, the concentration of salt was about 10 mM. The frequency of anodic events versus concentration curve for virus in a sample with 1 mM ferrocene methanol and 50 mM glucose is similar to the calculated curve (*SI Appendix*, Fig. S2) when mouse urine is spiked with a known amount of virus.

Interestingly, the collision frequency in urine may yield insight into the concentration of the virus as a function of the amount of time after which a host, which was a mouse in this study, was initially infected. Fig. 7 shows the frequency of collision from the urine analysis as a function of the time postinfection. Although MCMV is known to be shed in urine of infected animals, the kinetics and amplitude of this passing during a primary infection are not well characterized. From this plot, the virus was first observed 5 d postinfection. The shape of the curve correlates well with previously reported concentrations of infectious virus seen in the liver, spleen, and salivary glands from organ titers (23). This result implies that the electrochemical detection methodology proposed here may yield insight into the secretion of virus into the urinary system. The error bars on each measurement correspond to 10 measurements, which were taken over five different mice. Therefore, it is likely that the main source of imprecision is from the variability in physiology between mice. The frequency of collision events on day 5 implies that the limit of detection is about a 30-fM virion particle relying on diffusion alone. This number might be pushed to lower limits by increasing mass transfer.

In summation, we have presented a facile and direct electrochemical method for the detection of CMV at very low concentrations within a half hour of obtaining a urine sample. Our results indicate that specificity can be achieved by the antibody–epitope interaction, and the amplification of the electrochemical signal is achieved by the conjugation of the GOx enzyme to the primary neutralizing antibody. Because one GOx enzyme cannot produce enough current to show a discrete step in the amperometric i-t response, a type of preconcentration of GOx enzymes must be used to amplify the signal. The virus serves as a type of template around which GOx enzymes can preconcentrate, and this interaction is made highly specific by using a primary antibody that only recognizes glycoproteins on CMV. Anodic current steps only occur when a virus

is surrounded by enough GOx to catalyze the reaction near the electrode surface.

The collision experiments in urine demonstrated that the lowest concentration of virus particle detected was 30 fM. Generally, the signal-to-noise ratio of the detection ranged between 10 and 20. Moreover, the immunoassay also showed the capability of detecting a virus in urine 5 d after infection. The methods described here could be broadly applicable to other virus systems where primary antibody to a viral surface antigen is available; however, the size of the virus is likely important because a critical number of enzymes is required to achieve signal amplification.

Methods

Chemicals. Ferrocene methanol (98%) was purchased from Sigma-Aldrich. Solutions of ferrocene methanol were prepared by sonicating the solution for at least 20 min to dissolve ferrocene. This solution as then passed through a 100-nm pore filter. Glucose was purchased from Fisher Scientific and used without further purification. In each case, nanopure water was used for the experiments.

Electrochemistry. Electrochemical experiments were performed using a CHI model 900B potentiostat (CH Instruments). The three-electrode cell was placed in a faraday cage and grounded to a pipe. An Ag/AgCl (1 M KCl) wire was used (BASi) as the reference electrode, and a Pt wire was used as the auxiliary electrode.

Electrode Fabrication. The Pt UME was prepared following the general procedure developed in our laboratory (24). Electrodes were fabricated using a laser puller (Sutter Instruments) followed by a soft mechanical polishing until the electrode was 0.5–3 μm in radius. Briefly, a 25-μm-diameter Pt wire was placed in a glass capillary pulled to nanometer dimensions after a laser pulse locally heated and melted the glass and Pt. This electrode was then mechanically polished to the necessary size.

GOx Conjugation. GOx was covalently attached to purified anti-gB neutralizing antibody. Briefly, MCMV gB antibody, Mab97.3 kindly provided by Michael Mach, University of Erlangen, Erlangen, Germany, was purified from supernatant by way of affinity purification using agarose beads conjugated to protein A/G (Santa Cruz). Purified antibody was eluted from the protein A/G beads with 0.15% TFA. The elution solvent was removed via vacuum concentration (Speed Vac; Thermo Fisher) and resuspended in 1× PBS (137 mM NaCl, 2.7 mM KCl, 10 mM Na_2HPO_4, and 1.8 mM KH_2PO_4). Antibody concentration was determined via Bradford assay. The conjugation reaction was performed using a Glucose Oxidase Conjugation Kit (ab102887; Abcam) as per the manufacturer's instructions. The conjugate was incubated in the electrochemical samples for 30 min at 4 °C.

Virion Purification. Both MCMV and MHV68 virions were prepared as previously described (16). Briefly, concentrated virus was resuspended in complete DMEM supplemented with 10% (vol/vol) bovine calf serum, layered over 20% (wt/vol) sucrose cushion, and centrifuged 60 min at 32,800 × *g*. Pelleted virus was resuspended in Tris-buffered saline (0.05 M Tris and 0.10 M NaCl, pH 7.4), placed onto a 20–70% (wt/vol) continuous linear sorbitol gradient, and subjected to ultracentrifugation at 70,000 × *g* for 60 min at 16 °C. The virion band was visualized using light scatter from an overhead light source and collected by needle aspiration. Samples were subjected to a second round of ultracentrifugation to remove additional contaminants.

Animal Infections. C57BL/6J mice were infected with 10^6 pfu of WT MCMV via i.p. route of infection. Urine collection was performed at 3, 5, 7, 10, and 14 d postinfection. Control mice were infected with media only. Animals were maintained by the Animal Resources Center (ARC) at the University of Texas at Austin in accordance with Institutional guidelines, and all procedures were approved by the University of Texas at Austin Institutional Animal Care and Use Committee.

CHEMISTRY

MICROBIOLOGY

1. Xiao X, Bard AJ (2007) Observing single nanoparticle collisions at an ultramicroelectrode by electrocatalytic amplification. *J Am Chem Soc* 129(31):9610–9612.
2. Kim B-K, Boika A, Kim J, Dick JE, Bard AJ (2014) Characterizing emulsions by observation of single droplet collisions–Attoliter electrochemical reactors. *J Am Chem Soc* 136(13): 4849–4852.
3. Dick JE, Renault C, Kim B-K, Bard AJ (2014) Simultaneous detection of single attoliter droplet collisions by electrochemical and electrogenerated chemiluminescent responses. *Angew Chem Int Ed Engl* 53(44):11859–11862.
4. Cheng W, Compton RG (2014) Investigation of single-drug-encapsulating liposomes using the nano-impact method. *Angew Chem Int Ed Engl* 53(50):13928–13930.
5. Lebègue E, Anderson CM, Dick JE, Webb LJ, Bard AJ (2015) Electrochemical detection of single phospholipid vesicle collisions at a Pt ultramicroelectrode. *Langmuir* 31(42): 11734–11739.
6. Dick JE, Renault C, Bard AJ (2015) Observation of single-protein and DNA macro-molecule collisions on ultramicroelectrodes. *J Am Chem Soc* 137(26):8376–8379.
7. Dick JE, Bard AJ (2015) Recognizing single collisions of $PtCl_6^{2-}$ at femtomolar concentrations on ultramicroelectrodes by nucleating electrocatalytic clusters. *J Am Chem Soc* 137(43):13752–13755.
8. Bard AJ, Zhou H, Kwon SJ (2010) Electrochemistry of single nanoparticles via electrocatalytic amplification. *Isr J Chem* 50:267–276.
9. Goodman AL, Murray CD, Watkins J, Griffiths PD, Webster DP (2015) CMV in the gut: A critical review of CMV detection in the immunocompetent host with colitis. *Eur J Clin Microbiol Infect Dis* 34(1):13–18.
10. Ligozzi M, Poggi M, Saletti M, Gibellini D (2016) Development of a real-time quantitative polymerase chain reaction assay for the detection of congenital human cytomegalovirus infection in urine samples. *Mol Cell Probes* 30(1):50–52.
11. Kaushik A, Tiwari S, Dev Jayant R, Marty A, Nair M (2016) Towards detection and diagnosis of Ebola virus disease at point-of-care. *Biosens Bioelectron* 75:254–272.
12. Reddehase MJ (2002) Antigens and immunoevasins: Opponents in cytomegalovirus immune surveillance. *Nat Rev Immunol* 2(11):831–844.
13. Carlson A, Norwitz ER, Stiller RJ (2010) Cytomegalovirus infection in pregnancy: Should all women be screened? *Rev Obstet Gynecol* 3(4):172–179.
14. Heller A, Feldman B (2008) Electrochemical glucose sensors and their applications in diabetes management. *Chem Rev* 108(7):2482–2505.
15. Dick JE, Hilterbrand AT, Boika A, Upton JW, Bard AJ (2015) Electrochemical detection of a single cytomegalovirus at an ultramicroelectrode and its antibody anchoring. *Proc Natl Acad Sci USA* 112(17):5303–5308.
16. Bourdillon C, Demaille C, Gueris J, Moiroux J, Saveant JM (1993) A fully active monolayer enzyme electrode derivatized by antigen-antibody attachment. *J Am Chem Soc* 115(26): 12264–12269.
17. Bourdillon C, Demaille C, Moiroux J, Saveant JM (1993) New insights into the enzymatic catalysis of the oxidation of glucose by native and recombinant glucose oxidase mediated by electrochemically generated one-electron redox cosubstrates. *J Am Chem Soc* 115(1):2–10.
18. Quinn BM, Van 't Hof PG, Lemay SG (2004) Time-resolved electrochemical detection of discrete adsorption events. *J Am Chem Soc* 126(27):8360–8361.
19. Boika A, Thorgaard SN, Bard AJ (2013) Monitoring the electrophoretic migration and adsorption of single insulating nanoparticles at ultramicroelectrodes. *J Phys Chem B* 117(16):4371–4380.
20. Fosdick SE, Anderson MJ, Nettleton EG, Crooks RM (2013) Correlated electrochemical and optical tracking of discrete collision events. *J Am Chem Soc* 135(16):5994–5997.
21. Kwon SJ, et al. (2011) Stochastic electrochemistry with electrocatalytic nanoparticles at inert ultramicroelectrodes–Theory and experiments. *Phys Chem Chem Phys* 13(12): 5394–5402.
22. Einstein A (1905) Über die von der molekularkinetischen Theorie der Wärme geforderte Bewegung von in ruhenden Flüssigkeiten suspendierten Teilchen. *Ann Phys* 322:549–560.
23. Upton JW, Kaiser WJ, Mocarski ES (2012) DAI/ZBP1/DLM-1 complexes with RIP3 to mediate virus-induced programmed necrosis that is targeted by murine cytomegalovirus vIRA. *Cell Host Microbe* 11(3):290–297.
24. Fan F-RF, Demaille C (2001) The preparation of tips for scanning electrochemical microscopy. *Scanning Electrochemical Microscopy*, eds Mirkin MV, Bard AJ (Dekker, New York), 2nd Ed, pp 75–78.